JOURNAL OF Materials CHEMISTRY

Study on the Ti and Al coincorporation into the MFI zeolitic structure

G. Ovejero,* R. van Grieken, M. A. Uguina, D. P. Serrano and J. A. Melero

Department of Chemical Engineering, Faculty of Chemistry, Complutense University of Madrid, 28040 Madrid, Spain, E-mail: rada@eucmax.sim.ucm.es

Received 18th March 1998, Accepted 9th July 1998

The coincorporation of Ti and Al into the MFI zeolite framework has been investigated using a method based on the wetness impregnation of amorphous Al_2O_3–TiO_2–SiO_2 solids with TPAOH solutions and subsequent crystallization under autogenous pressure. The influence of the precursor addition sequence and the conditions during the amorphous cogel formation on the properties of the zeolites obtained have been studied. The Al content in the synthesized zeolite is similar to that of the raw cogel, whereas the Ti content is lower and depends on the degree of Al incorporation in the starting material. The distribution of Al and Ti in the Al-TS-1 samples depends not only on the initial Al content but also on the procedure to prepare the raw cogel. The activity for oxidation process of the Al-TS-1 samples prepared has been tested in *n*-hexane oxidation. The progressive incorporation of Al into the framework increases the oxidation capacity of Ti atoms compared to TS-1 until a maximum is reached (Al/Ti molar ratio: 0.70) whereas further Al incorporation decreases the catalytic activity to even lower values than in TS-1. This effect has been assigned to changes in the hydrophilic/hydrophobic character of the catalyst caused by the interaction between Al and Ti centers, which strongly affects the affinity towards the different compounds in the reaction mixture.

1 Introduction

Since the discovery of TS-1 as a suitable catalyst in selective oxidation reactions using hydrogen peroxide,[1–7] there have been several reports about the incorporation of other ions along with Ti^{4+} to modify the catalytic properties. Several studies have been reported recently[8–12] concerning the synthesis of zeolites containing both titanium and a trivalent element (Al^{3+}, Ga^{3+}, Fe^{3+} and B^{3+}) in MFI and MEL structures. The simultaneous presence of Ti and trivalent elements in lattice positions provides catalysts possessing activity in both oxidizing and acid-catalyzed reactions.

The methods reported in the literature for Al-TS-1 preparation[8–10] are based on the hydrothermal crystallization of a fluid gel obtained from respective precursors by basic hydrolysis with aqueous tetrapropylammonium hydroxide (TPAOH). An alternative and simpler method has been developed in our laboratory based on previous works on TS-1 synthesis by wetness impregnation of amorphous TiO_2–SiO_2 solids.[13–15] The use of the sol–gel route to prepare the raw solids has allowed us to obtain materials with high homogeneity and to control their composition and properties. In a separate paper,[12] we have described the method to incorporate simultaneously Al and Ti in the MFI framework, using as raw material Al_2O_3–TiO_2–SiO_2 cogels where Ti—O—Si and Al—O—Si bonds have been formed previously to the zeolite crystallization. The bifunctional properties of the material obtained have been applied in the MTBE preparation from isobutane (2-methylpropane) and methanol at 80–100 °C on a single catalytic system through both oxidizing and acid-catalyzed steps.[16] Additionally, several papers have been published about the use of these bifunctional materials (in particular Al-Ti beta and Ti-MCM41) in different processes where oxidant and acid centers are needed.[17,18]

In the preparation of multicomponent silicates following the sol–gel route,[19] it is widely accepted that one of the most convenient procedures is the sequential addition of the different alkoxides in the reverse order of their respective reactivities (least reactive precursor first) with a partial hydrolysis step after each addition. Thus, the newly added unhydrolyzed alkoxides will condense with partially hydrolyzed sites of the polymeric species formed in the preceding hydrolysis steps (heterocondensation). Then, an important factor to bear in mind is the sequential order of precursor addition and how it could affect the properties of the zeolites obtained by this procedure.

In this type of bifunctional catalyst, the presence of a third element in the zeolite could modify the activity of the different centers.[8,20,21] Therefore we were interested in studying some relevant aspects related to the influence of Ti and Al atoms not only in the coincorporation of both elements into the Al-TS-1 framework but also in the catalytic activity of the resulting materials.

2 Experimental

2.1 Sample preparation

Al-TS-1 samples. *Sample* 1. The Al_2O_3–TiO_2–SiO_2 solid used as raw material for the Al-TS-1 synthesis was prepared following a two step sol-gel process described elsewhere.[12] Tetraethylorthosilicate (TEOS, Alfa; 16 g) was first prehydrolyzed in an acid medium (10 g of 0.2 M HCl) before the addition of aluminium isopropoxide (AIP, Aldrich). Once the pH of the mixture was increased by dropwise addition of a 20 wt.% aqueous tetrapropylammonium hydroxide solution (TPAOH, Alfa; 0.1 g of aqueous TPAOH solution per g of TEOS), a solution of titanium butoxide (TNBT, Alfa; 0.65 g) in isopropyl alcohol was added slowly. Finally, the gelation was accelerated by further addition of 20 wt.% aqueous TPAOH solution (0.25 g of aqueous TPAOH solution per g of TEOS) and the cogel so obtained dried and crushed to give a powdered material.

Al-TS-1 was synthesized by thermal treatment under autogenous pressure of the wetness impregnated cogel with aqueous TPAOH solution (1.6 g TPAOH aqueous solution per g of dried cogel). The Al_2O_3–TiO_2–SiO_2 cogel was prepared with $SiO_2/TiO_2 = 40$ and $SiO_2/Al_2O_3 = 160$ molar ratios respectively. After impregnation, the incipient wet Al_2O_3–TiO_2–SiO_2 cogel was charged into Teflon-lined autoclaves and crystallized under autogenous pressure and static conditions at 170 °C for 24 h. The crystalline product of the synthesis was separated by centrifugation, washed several

times with distilled water, dried overnight at 110 °C and finally calcined in air at 550 °C for 7 h.

Sample 2. This sample was synthesized using an Al_2O_3–TiO_2–SiO_2 cogel ($SiO_2/TiO_2=40$ and $SiO_2/Al_2O_3=160$ molar ratios) prepared omitting the neutralization step before adding the titanium source. The remainder of the procedure is analogous to that of sample 1.

Sample 3. This sample was synthesized using an Al_2O_3–TiO_2–SiO_2 cogel ($SiO_2/TiO_2=40$ and $SiO_2/Al_2O_3=160$ molar ratios) prepared changing the alkoxide addition sequence (TNBT was added before AIP) and omitting the neutralization step before adding the titanium source. The remainder of the procedure is analogous to those of samples 1 and 2.

Samples 4–12. These Al-TS-1 samples were synthesized by thermal treatment of the wetness impregnated cogels with aqueous 20 wt.% TPAOH solution, except when the Al content was high ($SiO_2/Al_2O_3<160$), for which 30 wt.% TPAOH solution was used.

Eight Al_2O_3–TiO_2–SiO_2 cogels were prepared according to the recipe of sample 1 but with different molar compositions ($SiO_2/TiO_2=40$, 60 and 80 and $SiO_2/Al_2O_3=160$, 240 and 320 molar ratios, respectively). Additionally a cogel has been prepared with a higher Al content ($SiO_2/TiO_2=40$ and $SiO_2/Al_2O_3=120$ molar ratios). The synthesis conditions and product recovery of these samples are analogous to those of samples 1,2 and 3.

TS-1 sample. TS-1 was synthesized using as raw material amorphous SiO_2–TiO_2 solids prepared by the sol–gel process.[13–15] The amorphous solid was prepared omitting the AIP addition and the neutralization step while the remainder of the procedure is analogous to that of Al-TS-1 samples.

HZSM-5. HZSM-5 ($SiO_2/Al_2O_3=60$ molar ratio) was prepared according to the procedure initially developed by Person *et al.*[22] to synthesize silicalite-1. This method allows to obtain H-ZSM5 with a crystal size around 0.1–0.2 μm. The procedure is as follows: aluminium isopropoxide (AIP, Aldrich) was added to a tetraethylorthosilicate solution (TEOS/AIP mass ratio = 30.5) and the mixture stirred at 0 °C to obtain a clear solution. Then, 20 wt.% aqueous solution of TPAOH and water were added (20 wt.% TPAOH/H_2O mass ratio = 2.5), this final mixture being stirred for 12 h at room temperature. Thereafter the solution was heated to remove the alcohols and the liquid gel so obtained charged into a Teflon-lined autoclave and crystallized under autogenous pressure and static conditions at 170 °C for 3 days. The crystalline product was separated by centrifugation, washed several times with distilled water and dried overnight at 110 °C. The dried product was calcined in air at 550 °C during 7 h and finally the calcined sample exchanged with 0.2 M HCl and recalcined.

2.2 Characterization

Chemical analyses were performed by X-ray fluorescence (XRF) with a Philips PW 1480 spectrometer. X-Ray diffraction (XRD) patterns were collected with a Philips X'pert diffractometer with Cu-Kα radiation. Crystallinity was determined from the peak area between $2\theta=22$–$25°$ using a highly crystalline TS-1 sample as reference. FTIR spectra were recorded by means of a Nicolet 510P spectrophotometer using the KBr wafer technique. Diffuse reflectance UV–VIS spectra (DR UV–VIS) were obtained under ambient conditions on a CARY-1 spectrophotometer equipped with a diffuse reflectance accessory.

Chemical analyses of the crystal surface were carried out by X-ray photoelectron spectroscopy (XPS) with an Escalab 200R spectrometer equipped with an Mg-Kα 120 W X-ray source ($h\nu=1253.6$ eV). The samples were pressed into small aluminium cylinders and then mounted on a sample rod, placed in a pre-treatment chamber and outgassed at room temperature for 1 h prior to being transferred to the analysis chamber. The pressure in the ion-pumped analysis chamber was below 3×10^{-9} Torr during data acquisition. The spectra were collected for 20–90 min, depending on the peak intensities, at a pass energy of 10 eV. The intensities were estimated by calculating the integral of each peak after smoothing and subtraction of the S-shaped background and fitting the experimental curve to a combination of Gaussian and Lorentzian lines of variable proportion. All the binding energies (E_b) were referenced to the Si 2p signal at 103.4 eV.

Ammonia temperature programmed desorption (TPD) was carried out with a Micromeritics TPD/TPR 2900 apparatus. The sample was first outgassed by thermal treatment, from ambient temperature to 560 °C at a heating rate of 15 °C min^{-1} in a He stream (80 ml min^{-1}). After cooling to 200 °C, the sample was saturated with an NH_3 stream and consequently treated with a He stream (80 ml min^{-1}) for 90 min. Finally, the temperature is increased to 560 °C with a heating rate of 15 °C min^{-1} while recording NH_3 desorption with a thermal conductivity detector.

Competitive adsorption experiments for the determination of modified hydrophobicity index values were carried out with a fixed bed adsorber at atmospheric pressure using a method described in the literature.[23] The sample was first outgassed by thermal treatment from ambient temperature to 450 °C with a heating rate of 5 °C min^{-1} in a extrapure dry helium stream with a flow rate of 100 cm^3 min^{-1} and kept at this temperature for 1 h. An extrapure dry He stream with a flow rate of 12 cm^3 min^{-1} was passed through two saturators one of them held at 0 °C and filled with *n*-hexane (partial pressure: 0.9 kPa) and the other held at 25 °C and filled with water (partial pressure: 1.6 kPa). This mixture of water and *n*-hexane vapours was passed through the sample, which was previously cooled to room temperature. Typically *ca.* 0.5–0.6 g of adsorbent was used. The gas stream leaving the adsorber was analyzed continuously using a quadrupole mass spectrometer (Hiden analytical) equipped with a gas analyzer which allows breakthrough curves to be obtained with good accuracy. The final loadings (L_i) were calculated directly from the measured breakthrough curves and the modified hydrophobicity index (HI) was then calculated as the mass ratio between *n*-hexane and water adsorbed on the sample (L_{hexane}/L_{water}) in equilibrium with the gas stream containing both components.

Morphology and size of the crystallites were determined from scanning electronic microscopy (SEM) images taken with a JEOL JSM-6400 microscope. ^{29}Si and ^{27}Al MAS NMR spectra of powdered samples were recorded at 79.49 and 104.26 MHz, respectively, in a Bruker spectrometer Model MSL-400 equipped with a Fourier transform unit. The spinning frequency was 4000 Hz and time intervals of 5 s between successive accumulations were selected. Measurements were conducted at room temperature with tetramethylsilane (TMS) and $[Al(H_2O)_6]^{3+}$ as external standard references, with accumulations amounted to 2000 and 400 FIDs, respectively.

The catalytic tests of *n*-hexane oxyfunctionalization were carried out in a magnetically stirred batch reactor equipped with a temperature controller and pressure gauge. All the reactants and the catalyst were charged into the Teflon-lined reactor and the system was heated to 100 °C. Aqueous H_2O_2 (30 wt.% Panreac) was used as oxidant and methanol as solvent (H_2O_2/n-C_6 molar ratio = 1.176, *n*-C_6/methanol mass ratio = 0.276, *n*-C_6/catalyst mass ratio = 24–12 and mass catalyst = 0.1–0.2 g). The H_2O_2 concentration after reaction was evaluated by iodometric titration. The catalytic test for acid-catalyzed reactions [*tert*-butyl alcohol(2-methylpropan-2-ol)

and methanol etherification] were carried out in analogous stirred autoclaves. *tert*-Butyl alcohol, methanol and the required amount of catalyst were charged into the Teflon-lined autoclave (*tert*-butyl alcohol/methanol mass ratio = 0.1, *tert*-butyl alcohol/catalyst mass ratio = 2.5 and catalyst mass = 0.4 g) and then the system was heated to 100 °C. All the reaction products were analyzed by gas chromatography (Varian 3400) on a capillary column, DV1 methylsilicone (60 m × 0.02 mm).

3 Results and discussion

3.1 Comparison among different cogel preparation methods

Samples 1, 2 and 3 have been synthesized from previously described amorphous Al_2O_3–TiO_2–SiO_2 cogels (SiO_2/TiO_2 = 40 and SiO_2/Al_2O_3 = 160) wetness impregnated with the template solution. The three cogels were impregnated with the same quantity of TPAOH solution (1.6 g of 20 wt.% aqueous solution/1 g dried cogel) and the hydrothermal crystallization was carried out at 170 °C for 24 h under autogenous pressure and static conditions. In the three samples, high synthesis yields were obtained (> 95 wt.%) on the basis of SiO_2 content in the initial cogel.

In the three samples, materials with MFI structure and high crystallinity were obtained as concluded from XRD measurements and all samples show orthorhombic symmetry. The crystal size (d) of the samples determined by SEM is similar for the three samples ranging from 0.4–0.5 μm.

The chemical analyses performed by XRF of the zeolites samples are shown in Table 1. The Ti and Al content in the three samples is very similar, the Si/Al molar ratio in all being very close (around 80) to that in the raw material (amorphous cogel), whereas the Si/Ti molar ratio is higher, likely due to the competition between Al and Ti for incorporation into the zeolitic framework.[8,12] XPS measurements of the calcined samples give the binding energies for Ti $2p_{3/2}$ listed in Table 1. The binding energies are around 460 eV, close to 460.2 reported by Carati *et al.* for TS-1[24] and also to the value of 459.8 eV reported for TS-2.[25] Additionally, this high value of binding energy is a strong indication that in all three samples the Ti atoms have a tetrahedral environment.[26] The surface chemical analysis of the Al-TS-1 crystals (samples 1, 2 and 3) shown in Table 1 indicates a slight decrease in the Ti content in the outer shell of the crystals, this decrease being more pronounced for sample 3. Additionally, it should be noted that in samples 1 and 2, in which AIP is added first, the Al is almost uniformly distributed, whereas in sample 3 a very high concentration of Al is observed in the outer shell of the crystals. These concentration gradients seem to be influenced by the addition sequence of the different alkoxides and therefore the procedure used to prepare the raw cogel has an important influence on the composition gradients of the final synthesized material.

The IR spectra of the Al-TS-1 samples show a band at 960 cm^{-1} related to the stretching vibration of Si—O bonds adjacent to framework Ti atoms.[27] The relative intensity of this band, I_{960}/I_{800}, correlates well with the Ti content in the zeolite framework.[28] As shown in Table 1, the relative intensity of this band is very similar for the three samples which suggests, at first sight, a similar degree of Ti incorporation into the crystalline structure. In the DR UV–VIS spectra of the three Al-TS-1 samples shown in Fig. 1, no absorption around 330 nm is detected and a narrow band for all three samples is centred around 210 nm, confirming that the Ti atoms occupy tetrahedral positions in the zeolite framework,[29] which is in accord with the values of binding energies for Ti $2p_{3/2}$ obtained from XPS measurements. However, it is not possible to completely discount the presence of a very small amount of TiO_2 rich micro-domains.

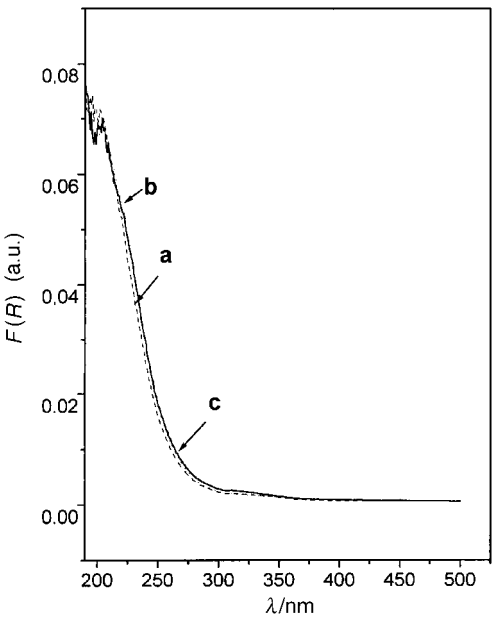

Fig. 1 DR UV–VIS spectra of calcined Al-TS-1 samples: (a) sample 1, (b) sample 2, (c) sample 3.

^{27}Al MAS NMR spectra of the calcined Al-TS-1 samples show a peak at 52 ppm assigned to the presence of Al atoms in tetrahedral positions.[30] Although samples 1 and 3 show basically only this feature, sample 2 clearly shows another small sharp peak at 0 ppm (Fig. 2) which is indicative of the presence of extraframework Al in octahedral coordination.[30] TPD analysis shows a similar NH_3 adsorption capacity and acid strength for samples 1 and 3, but sample 2 presents a somewhat lower NH_3 adsorption capacity (Table 1).

The results obtained with the Al-TS-1 samples in the catalytic experiments of n-C_6 oxidation with H_2O_2 and methanol/*tert*-butyl alcohol etherification are given in Table 2. Samples 1 and 3 exhibit very high activity and H_2O_2 selectivity for the conversion of n-C_6 into a mixture of hexan-2- and -3-ols and hexanones and a good catalytic activity and selectivity for the etherification reaction in good accord with the similar characterization results obtained by XRF, DR UV–VIS, IR, TPD and MAS NMR. However, it should be noted that samples 1 and 3 show very different concentration gradients within the crystals (Table 1), but this has no influence on the bifunctional catalytic activity. This is probably attributable to the small particle size of the samples, which allows a very fast

Table 1 Molar composition and properties of Al-TS-1 samples

	Bulk composition			Surface composition						
Sample	SiO_2	TiO_2	Al_2O_3	SiO_2	TiO_2	Al_2O_3	I_{960}/I_{800}[a]	d/μm	TPD[b]	E_b (Ti $2p_{3/2}$)[c]/eV
1	76	1	0.48	90	1	0.48	1.36	0.4–0.5	0.17	460.0
2	80	1	0.50	90	1	0.54	1.32	0.4–0.5	0.13	460.0
3	80	1	0.50	100	1	0.94	1.35	0.4–0.5	0.16	459.8

[a]Ratio between the intensities, in absorbance units, of the 960 and 800 cm^{-1} IR bands. [b]NH_3 adsorption capacity (mmol g^{-1}) [c]Binding energy from XPS measurements.

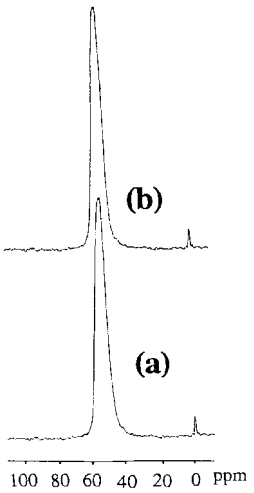

Fig. 2 ^{27}Al MAS NMR spectra of calcined Al-TS-1 samples: (a) unexchanged sample 2, (b) acid exchanged sample 2.

internal diffusion through the zeolite pores and hence the presence of the composition gradient does not influence the catalytic performance of the samples. In contrast, sample 2 presents a somewhat lower activity and H_2O_2 selectivity in the oxidation reaction, while a decrease is also observed in the *tert*-butyl alcohol conversion for the etherification reaction although its composition gradient is very similar to sample 1. These differences can be related to the presence of extraframework Al not incorporated in sample 2 as supported by the presence of Al in octahedral coordination (Fig. 2). The sharpness of the peak in the ^{27}Al MAS NMR spectrum could be associated with a very small particle size of alumina or Al^{3+} cations at exchangeable positions. In order to assign the origin of this signal at 0 ppm, sample 2 was exchanged with an aqueous solution of HCl at room temperature for 6 h to remove Al^{3+}. The ^{27}Al MAS NMR of exchanged sample 2 show that the signal at 0 ppm is still present after the acid treatment [Fig. 2(b)], which confirms the presence of very small extraframework Al_2O_3 particles rather than Al^{3+} cations. These species are probably placed within the channel system of the zeolite, which leads to a decrease in the NH_3 adsorption capacity and a decrease in the activity of the sample due to diffusional restrictions, with an increase in the decomposition of H_2O_2.

The procedure used to prepare the cogel corresponding to sample 1 is based on the sequential addition of the different alkoxides in the reverse order of their respective reactivities.[19] Following this technique, AIP was added before TNBT, the former being hydrolyzed in a highly acidic medium to favour the hydrolysis step. Before TNBT addition, a 20 wt.% aqueous solution of TPAOH is added to reach a similar pH to that corresponding to the preparation of TiO_2–SiO_2 cogels.[13–15] Although a concise possible explanation is difficult, the different pH conditions during the preparation of the three cogels (mainly the aluminium addition step) leads to aluminium species with different reactivity for incorporation into the silica colloidal particles.[19]

3.2 Effect of the Ti and Al contents in the raw xerogel

Several Al_2O_3–TiO_2–SiO_2 solids were prepared following a method similar to that of sample 1 with Si/Ti molar ratios varying between 40 and 80, and Si/Al molar ratios varying between 60 and 160. The zeolite synthesis were carried out by wetness impregnation of these cogels with the same amount

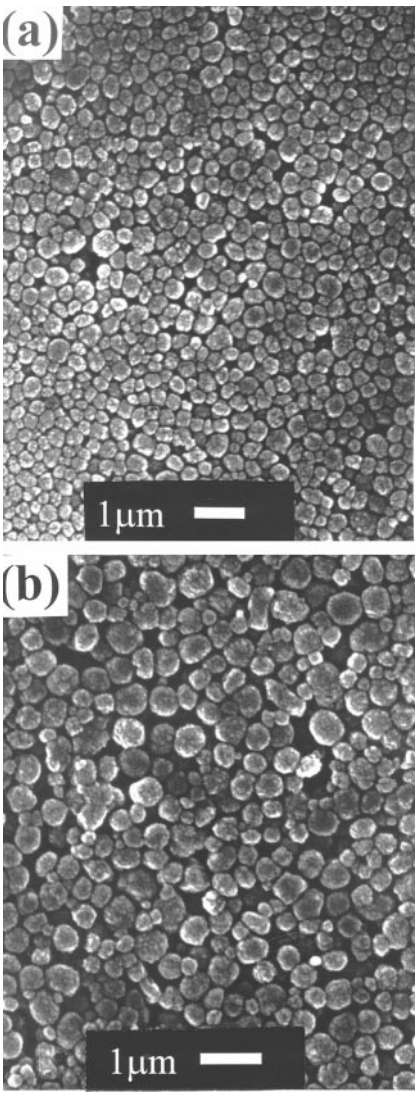

Fig. 3 SEM images of different calcined Al-TS-1 samples: (a) sample 1, (b) sample 4.

Table 2 Catalytic properties of Al-TS-1 samples

	n-hexane oxidation[a]			Alcohol etherification[b]	
Sample	*n*-hexane conversion (%)	H_2O_2 conversion (%)	H_2O_2 selectivity[c] (%)	*tert*-butyl alcohol conversion (%)	MTBE selectivity[d] (%)
1	65	85	96	75	97
2	58	88	83	67	97
3	63	89	97	77	95

[a]Reaction conditions: $T = 100\,^{\circ}C$, $t = 1$ h. Composition of the reaction mixture: $H_2O_2/n\text{-}C_6$ mole ratio = 1.176, $n\text{-}C_6$/methanol mass ratio = 0.276, $n\text{-}C_6$/catalyst mass ratio = 12 and catalyst mass = 0.2 g. [b]Reaction conditions: $T = 100\,^{\circ}C$, $t = 2$ h. Composition of the reaction mixture: *tert*-butyl alcohol/methanol mass ratio = 0.1, *tert*-butyl alcohol/catalyst mass ratio = 2.5 and catalyst mass = 0.4 g. [c] Selectivity defined as: (mol hexanols + 2 × mol hexanones obtained)/mol H_2O_2 converted. [d]Selectivity defined as: (mol MTBE obtained/mol *tert*-butyl alcohol converted).

Table 3 Properties and molar composition of Al-TS-1 samples and corresponding cogels

		Molar cogel composition		Molar sample composition		Physicochemical properties of the samples	
Sample	Type	SiO_2/TiO_2	SiO_2/Al_2O_3	SiO_2/TiO_2	SiO_2/Al_2O_3	I_{960}/I_{800}[a]	TPD[b]
1	Al-TS-1	40	160	76	160	1.36	0.17
4	Al-TS-1	40	120	89	120	1.10	0.24
5	Al-TS-1	40	240	73	236	1.44	0.12
6	Al-TS-1	40	320	57	317	1.55	0.10
7	Al-TS-1	60	160	90	160	1.42	0.18
8	Al-TS-1	60	240	92	239	1.45	0.12
9	Al-TS-1	60	320	73	319	1.57	0.10
10	Al-TS-1	80	160	89	160	1.34	0.17
11	Al-TS-1	80	240	91	240	1.34	0.12
12	Al-TS-1	80	320	90	320	1.35	0.10
13	TS-1	40	∞	49	∞	1.80	0.00
14	H-ZSM5	—	—	∞	60	—	0.45

[a]Ratio between the intensities, in absorbance units, of the 960 and 800 cm^{-1} IR bands. [b]NH_3 adsorption capacity in mmol g^{-1}.

of 20 wt.% aqueous TPAOH solution, except for the sample with the highest Al content (Si/Al = 60) which was impregnated with the same amount of 30 wt.% aqueous TPAOH solution. This difference is based on the results of previous experiments, which showed that when a xerogel with a high Al content is used as raw material, the concentration of the TPAOH solution must be increased in order to obtain zeolites with high crystallinity. The main properties of both cogel and zeolite samples are summarized in Table 3.

All the synthesized samples present a MFI structure and a high crystallinity as concluded from XRD measurements. Fig. 3 shows the SEM images of two different samples of Al-TS-1 (samples 1 and 4), showing crystals of homogeneous size and shape.

The chemical analysis by XRF shows that the Ti content in the Al-TS-1 samples is lower than in the TS-1 sample and in both cases lower than that corresponding to the raw cogel. On the other hand, the Al content in Al-TS-1 samples is similar to that in the raw cogel, independently of the Ti presence in the initial amorphous material. According to these results, the maximum amount of Ti incorporated into the framework appears to depend on the concentration of Al in the raw cogel. In order to assess this dependence, several cogels were prepared varying the Al content with a constant Ti content in the raw solid (samples 1,4,5,6 and 13; Table 3). TS-1 (sample 13) presents the highest Ti content close to that in the initial cogel, but as the amount of Al increases in the raw cogel, the amount of Ti incorporated into the zeolite starts to decrease (samples 1,4,5 and 6; Table 3). Chemical analysis of samples synthesized using as raw materials Al_2O_3–TiO_2–SiO_2 solids with medium (samples 7–9; Table 3) and low (samples 10–12; Table 3) Ti content, show that the Ti incorporation into the framework during the synthesis not only depends on the SiO_2/Al_2O_3 molar ratio in the initial cogel but also on the SiO_2/TiO_2 molar ratio. Thus, as Ti content decreases in the initial cogel, the proportion of Ti incorporated during the synthesis is higher, and at very low Ti content (samples 10–12, Table 3), the Al content in the raw material does not seem to influence the Ti incorporation.

This trend is clearly shown in Fig. 4 where the Ti content in zeolite is plotted *versus* Ti content in the raw material. All the values corresponding to different samples are below the diagonal which confirms that the initial amount of titanium in the xerogel is not completely incorporated into the framework during the synthesis. The presence of Al in the raw cogel lowers the incorporation of Ti in the zeolitic framework as was suggested in previous papers for Al-TS-1.[9,12] Any isomorphous substitution of a silicon atom in silicalite-1 leads to a degree of distortion of the framework which depends on the nature of the incorporated element. Thus, the synthesis of zeolites with

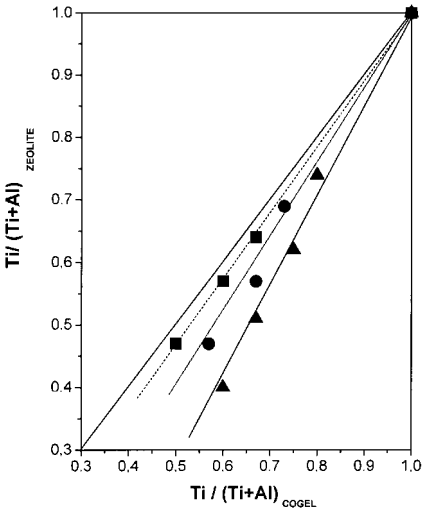

Fig. 4 Ti incorporation into the MFI structure from the starting cogel with SiO_2/TiO_2 molar ratios of: (▲) 40, (●) 60 and (■) 80.

MFI structure presents no problems for Si/Al molar ratios around 15 whereas this limit is around 40 for Si/Ti. Owing to the differences in the affinity towards isomorphous substitution between Al and Ti atoms, the aluminium present in the starting xerogel is completely incorporated during the synthesis limiting the maximum amount of Ti in the zeolite.

XPS measurements performed on the calcined samples 1,4,5 and 13, synthesized from cogels prepared varying the Al concentration and constant Ti content, have allowed determination of composition gradients in the final material. As can be seen in Table 4, there is a decrease in the Ti content on the outer surface of the crystals when Al is present and this decrease is more pronounced with higher Al content in the raw material. It should be also pointed out that Ti is uniformly distributed in TS-1 crystals synthesized by wetness impregnation (sample 13). The values of binding energies for Ti $2p_{3/2}$ listed in Table 4 indicate, for all the samples tested, that Ti atoms are located in a tetrahedral environment into the zeolite framework.[26]

Since the relative intensity of the band, I_{960}/I_{800}, in the IR spectra correlates well with the Ti content in the zeolite framework,[28] the values in Table 3 indicate a higher degree of Ti incorporation in TS-1 (sample 13) and a decrease in this ratio as the alumina content in the cogels increases, in good agreement with the XRF chemical analysis. DR UV–VIS spectra of all samples show only a narrow band centred around 210 nm confirming that the Ti atoms occupy tetra-

Table 4 Bulk and surface molar chemical composition determined by XPS of Al-TS-1 and TS-1 samples

	Bulk composition		Surface composition		Binding energy/eV	
Sample	SiO_2/TiO_2	SiO_2/Al_2O_3	SiO_2/TiO_2	SiO_2/Al_2O_3	Al 2p	Ti $2p_{3/2}$
4	89	120	111	86	74.1	460.0
1	76	160	90	188	74.5	460.0
5	73	236	77	200	74.2	459.9
13	49	∞	50	∞	—	459.8

hedral positions in the zeolite framework without presence of extraframework titanium species.[29] NH_3 adsorption capacity of the samples shows that TS-1 (sample 13) exhibits a negligible NH_3 adsorption capacity whereas Al-TS-1 samples show a capacity proportional to the aluminium incorporated, in close agreement with the theoretical Al content in the MFI structure.

3.3 Enhancement of catalytic activity of Ti induced by Al incorporation

The presence of different catalytic sites inside the zeolite channels makes interesting to investigate the possible interaction between them and their effect on the catalytic activity.

Table 5 shows the results obtained in the catalytic experiments of *n*-hexane oxidation with H_2O_2. All samples exhibit a high activity for the conversion of *n*-C_6 into a mixture of hexan-2- and -3-ols and hexanones with similar H_2O_2 selectivity, nearly 100% . For comparison, a sample of H-ZSM5 (sample 14), with a Si/Al molar ratio around 30 and with similar crystal size (0.1–0.2 μm), has been used in the oxidation test of *n*-hexane. Although the hydrogen peroxide decomposition is clearly enhanced with H-ZSM5, the oxidation activity due to Al atoms present in H-ZSM5 is surprising.[31] Assuming that the oxidation activity of Al atoms located in Al-TS-1 samples is similar to that in H-ZSM5, it is possible to estimate the accumulated turnover number corresponding to the contribution of Ti atoms on the global oxidation activity in Al-TS-1 samples (Table 5).

From comparison among the experiments carried out with samples 6, 9 and 12 with low Al content, it is observed that the higher the Ti content the lower the activity per Ti atom, in agreement with the low value obtained for TS-1 (2.64 wt.% TiO_2). However, when the comparison is made between samples 5, 8 and 11 (medium Al content) and samples 1,7 and 10 (high Al content), this behavior is no longer observed, since there is no significant change in the activity for samples with different TiO_2 content. Besides, sample 4 with the same titanium content of samples 7, 8, 10, 11 and 12 but higher Al content (1.37 wt.% of Al_2O_3) shows a remarkable decrease of the accumulated turnover number. All these experimental facts lead to the dependence of the oxidation activity, not on the TiO_2 content but on the Al/Ti molar ratio incorporated in the samples. Thus, if the oxidizing activity per Ti atom is plotted *vs.* the Al/Ti molar ratio in the catalyst framework (Fig. 5), it is readily observed that the presence of Al increases the activity of Ti atoms in Al-TS-1 with respect to that in TS-1 reaching a maximum for an Al/Ti molar ratio around 0.7. However, when the Al is increased beyond this molar ratio, the activity begins to decrease, eventually reaching even lower values than that for Ti atoms in TS-1. It is concluded from these results that the presence of Al in Al-TS-1 samples leads to a different activity per Ti atom for oxidation activity with respect to that in TS-1, with an optimum Al/Ti molar ratio around 0.7. A similar trend has been recently suggested for the oxidation of cyclohexene, using H_2O_2 as oxidant, catalyzed by Ti-beta.[21]

It has been proposed that due to the hydrophobicity of TS-1 the concentration of water surrounding the titanium is at a low level, which makes this material a very efficient catalyst for oxidation with aqueous H_2O_2.[32] On the other hand, the use of the modified hydrophobicity index (HI) as a quantitative measure for the hydrophobic/hydrophilic surface properties of molecular sieves has been used. In this context, Weitkamp *et al.* have thoroughly studied the competitive

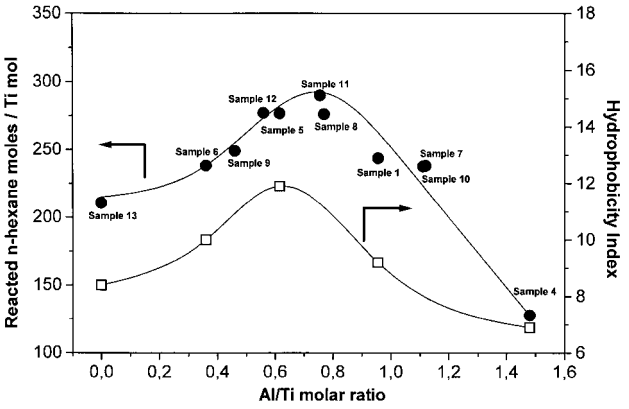

Fig. 5 Variation of both the catalytic activity for the *n*-hexane oxidation reaction (●) and hydrophobicity index (□) with the Al/Ti molar ratio.

Table 5 Activity of Al-TS-1 samples for *n*-hexane oxidation

Sample[a]	Type	SiO_2 (wt.%)	TiO_2 (wt.%)	Al_2O_3 (wt.%)	Al/Ti molar ratio	Reacted mol *n*-C_6 per mol Ti
13	TS-1	97.36	2.64	0	0	210.6
6	Al-TS-1	97.21	2.27	0.52	0.36	238.2
9	Al-TS-1	97.70	1.78	0.52	0.46	249.0
12	Al-TS-1	98.03	1.45	0.52	0.56	277.0
5	Al-TS-1	97.52	1.78	0.70	0.62	276.6
8	Al-TS-1	97.88	1.42	0.70	0.77	276.0
11	Al-TS-1	97.88	1.43	0.70	0.76	289.8
1	Al-TS-1	97.27	1.70	1.03	0.95	243.6
7	Al-TS-1	97.53	1.44	1.03	1.12	238.0
10	Al-TS-1	97.51	1.46	1.03	1.11	237.6
4	Al-TS-1	97.18	1.45	1.37	1.48	127.8
14	H-ZSM5	97.25	0	2.75	∞	14.4[b]

[a]Reaction conditions: $T = 100$ °C, $t = 10$ min. Composition of the reaction mixture: H_2O_2/*n*-C_6 mole ratio = 1.176, *n*-C_6/methanol mass ratio = 0.276, *n*-C_6/catalyst mass ratio = 24 and catalyst mass = 0.1 g. [b]Reacted moles *n*-C_6 per moles Al.

adsorption of vapour mixtures of an alkane and water on acid materials such as ZSM-5 [23] and more recently on TS-1.[33] From these results it was confirmed that the HI increases with the Si/Al molar ratio in acid materials and that the titanium silicalites adsorb more water than the titanium-free counterpart silicalite-1. The increase in the hydrophilic character with Ti content was attributed to the increased formation of polar Si—O—Ti bridges in the zeolite framework.[33] From these results it can be concluded that the hydrophilic character of these materials increases not only with the Al content but also with the Ti content and hence we decided to measure the HI for several TS-1 and Al-TS-1 samples and the resulting values are plotted in Fig. 5. As can be seen, the HI can be correlated with the Ti activity in the liquid phase oxidation of *n*-hexane with H_2O_2. In particular, as HI increases, the catalytic activity per Ti atom is enhanced. The progressive increase of HI favours the adsorption of the organic molecules on the catalyst surface instead of the water, leading to an enhancement of the catalytic activity in oxidation. On the contrary, low HI indicates preferential adsorption of water, which leads to a poorer performance of Ti centers for oxidation catalysis with aqueous H_2O_2. From these experimental results, it is concluded that a low concentration of Al atoms into the Al-TS-1 framework increases the hydrophobic character of the zeolite in comparison to TS-1 leading to a better performance in the oxidation of *n*-hexane with aqueous H_2O_2. This surprising result can be attributed to the modification of the electronic density around the Ti sites induced by the close presence of Al, changing their hydrophilic character and hence providing an increase of their intrinsic activity for oxidation. However, when the Al content is high (sample 4) this enhancement of the activity is overcome by the higher water adsorption instead of *n*-hexane which leads to a decrease of the catalyst activity. This interaction between Al and Ti atoms suggests their close proximity in the unit cell, as a consequence of the distortion caused by the isomorphous substitution of silicon by a first element and the generation of preferential sites for the incorporation of a second element.

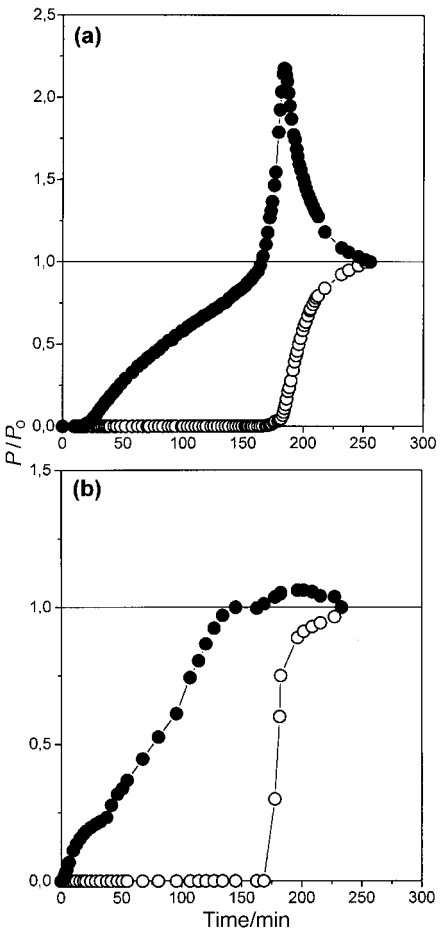

Fig. 6 Breakthrough curves in the competitive adsorption of vapour mixtures of *n*-hexane (○) and water (●). (a) Al-TS-1 (sample 1), (b) TS-1 (sample 13).

The breakthrough curves for TS-1 and Al-TS-1 samples were measured using a binary vapour mixture of *n*-hexane and water according to a method described in the literature.[23] Fig. 6(a) and (b) show the typical breakthrough curves for the competitive adsorption of sample 1 (Al-TS-1) and sample 13 (TS-1), respectively. It can be seen that water begins to break through soon after the start of the experiment. However a delay is observed in the Al-TS-1 samples in comparison to the TS-1 sample owing to the presence of highly hydrophilic Al atoms. After a time on stream of *ca.* 170 min, simultaneously with the *n*-hexane breakthroughs, a displacement of adsorbed water by *n*-hexane is observed which has also been reported for other Al containing materials.[23] However it must be pointed out that this displacement is much less pronounced in the TS-1 sample in comparison with Al-TS-1 samples.

4 Conclusions

The properties of Al-TS-1 samples depend on the method used to prepare the starting cogel according to the characterization and catalytic results obtained. The pH conditions present during the condensation of Al and Ti alkoxides play an important role in the Al species incorporation whereas the addition sequence has an influence on the composition gradients of the Al-TS-1 samples.

Not all the Ti present in the raw Al_2O_3-TiO_2-SiO_2 cogel is incorporated into the zeolite as it occurs in the synthesis of TS-1 by a similar procedure. However in Al-TS-1 the degree of incorporation of Ti is much lower than in TS-1, probably due to a competitive effect with Al species, which are incorporated completely into the framework during the synthesis. This effect also depends on the Ti content in the initial cogel, showing that at very low Ti content this dependence disappears and the degree of Ti incorporation into the framework becomes independent of the Al content. The Ti composition gradient within the crystals of Al-TS-1 also depends on the initial Al content of the raw xerogel. A decrease of Ti content on the outer shell is observed as the Al content in the raw material increases. However, Ti is uniformly distributed in the TS-1 sample synthesized by the wetness impregnation method.

The intrinsic catalytic activity of Ti sites in Al-TS-1 for alkane oxidation with H_2O_2 depends on the Al/Ti molar ratio incorporated into the zeolite lattice. The presence of Al in Al-TS-1 samples modifies the activity per Ti atom for oxidation in comparison to that in TS-1, with an optimum Al/Ti molar ratio of *ca.* 0.7. This optimum seems to be related with the changes in the hydrophilic/hydrophobic character of the catalytic samples determined by the Al/Ti molar ratio into the framework, which affects the affinity towards the different compounds of the reaction mixture.

Financial support by the Comisión Interministerial de Ciencia y Tecnología of Spain (Project MAT 96/0924) is gratefully acknowledged. We also thank CEPSA Research Centre for the XRF measurements, Drs. Jesus Sanz and Isabel Sobrados (CSIC, Spain) for the MAS NMR measurements and Dr. J. L. G. Fierro (CSIC, Spain) for the XPS measurements.

References

1 M. Taramasso, G. Perego and B. Notari, *US Pat.*, 4410501, 1983.
2 P. Roffia, M. Padovan, E. Moretti and G.D. Alberti, *Eur. Pat. Appl.,* 208311, 1987.

3 D. R. C. Huybrechts, L. D. Bruycker and P. A. Jacobs, *Nature,* 1990, **345**, 240.
4 A. Tuel, S. Moussa-Khouzami, Y. Ben Taârit and C. Naccache, *J. Mol. Catal.,* 1991, **68,** 45.
5 M. G. Clerici, G. Bellusi and U. Romano, *J. Catal.*, 1991, **129**, 159.
6 A. Thangaraj, R. Kumar and P. Ratnasamy, *J. Catal.,* 1991, **131**, 394.
7 B. Notari, *Catal. Today*, 1993, **18,** 163.
8 G. Bellusi, A. Carati, M. G. Clerici and A. Esposito, *Stud. Surf. Sci. Catal.*, 1991, **63**, 421.
9 L. Forni, M. Pellozi, A. Giusti, G. Fornasari and R. Millini, *J. Catal*., 1990, **122**, 44.
10 A. Thangaraj, R. Kumar and S. Sivasanker, *Zeolites*, 1992, **12**, 135.
11 D. Trong On, S. Kaliaguine and L. Bonneviot, *J. Catal.,* 1995, **157**, 235.
12 G. Ovejero, R. van Grieken, M. A. Uguina, D. P. Serrano and J. A. Melero, *Catal. Lett.,* 1996, **41**, 69.
13 M. A. Uguina, G. Ovejero, R. van Grieken, D. P. Serrano and M. Camacho, *J. Chem. Soc., Chem. Commun.*, 1994, 27.
14 D. P. Serrano, M. A. Uguina, G. Ovejero, R. van Grieken and M. Camacho, *Microporous Mater.*,1995, **4**, 273.
15 M. A. Uguina, D. P. Serrano, G. Ovejero, R. van Grieken and M. Camacho, *Appl. Catal. A,* 1995, **124**, 391.
16 R. van Grieken, G. Ovejero, D. P. Serrano, M. A. Uguina and J. A. Melero, *Chem. Commun.*, 1996, 1145.
17 A. Corma, M. Iglesias and F. Sanchez, *J. Chem. Soc.*, *Chem. Commun*., 1995, 1635.
18 M. van Klaveren and R. Sheldon, *Stud. Surf. Sci. Catal*., 1997, **110**, 567.
19 C. J. Brinker and G. W. Scherer, *Sol–Gel Science. The Physics and Chemistry of sol–gel processing*, Academic Press, London, 1990.
20 S. Gontier and A. Tuel, *J. Catal.,* 1995, **157**, 124.
21 A. Corma, M.A. Camblor, P. Esteve, A. Martínez and J. Pérez-Pariente, *J. Catal.,* 1994, **145**, 151.
22 A. E. Person, B. J. Schoeman, J. Sterte and J. E. Otterstedt, *Zeolites,* 1994, **14**, 557.
23 J. Weitkamp, P. Kleinschmit, A. Kiss and C. H. Berke, *Proceedings from the 9th International Zeolite Congress*, ed. R. von Ballmoos, J. B. Higgins and M. M. J. Treacy, Butterworth-Heinemann, Boston, 1992, vol. II, p. 79.
24 A. Carati, S. Contarini, R. Millini and G. Bellussi, *Mater. Res. Soc. Ext. Abstr.*, ACS Symposium of Synthesis and Properties of New Catalysts, Boston, 1990, p. 47.
25 D. Trong On, L. Bonneviot, A. Bittar, A. Sayari and S. Kaliaguine, *J. Mol. Catal*., 1992, **74**, 233.
26 S. M. Mukhopadhyay and S. H. Garofalini, *J. Non-Cryst. Solids,* 1990, **126**, 202.
27 M. A. Camblor, A. Corma and J. Pérez-Pariente, *J. Chem. Soc.*, *Chem. Commun.*, 1993, 557.
28 A. Thangaraj, R. Kumar, S. P. Mirajkar and P. Ratnasamy, *J. Catal.*, 1991, **130**, 1.
29 F. Geobaldo, S. Bordiga, A. Zecchina, E. Gianello, G. Leofanti and G. Petrini, *Catal. Lett.*, 1992, **16**, 109.
30 A. D. Irwin, J. S. Holmgren and J. Jonas, *J. Mater. Sci.*, 1988, **23**, 2098.
31 R. J. Sudhakar, U. R. Khire, P. Ratnasamy and R. B. Mitra, *J. Chem. Soc.*, *Chem. Commun.*, 1992, 1234.
32 C. B. Khouw, C. B. Dartt, J. A. Labinger and M. E. Davis, *J. Catal.,* 1994, **149**, 195.
33 J. Weitkamp, S. Ernst, E. Roland and G. F. Thiele, *Stud. Surf. Sci. Catal.*, 1997, **105**, 763.

Paper 8/02146E